frontiers in Materials

ORIGINAL RESEARCH
published: 21 April 2020
doi: 10.3389/fmats.2020.00080

Preparation and Microwave Absorption Properties of Ni_xS_y/PVDF Nanocomposites

Yu-Hui Du[1], Na Gao[2], Mao-Dong Li[1], Lei Wang[3] and Guang-Sheng Wang[2]**

[1] Guangzhou Special Pressure Equipment Inspection Institute, Guangzhou, China, [2] School of Chemistry, Beihang University, Beijing, China, [3] Beijing Institute of Technology, Zhuhai, China

Octahedral Ni_xS_y nanoparticles and Ni_xS_y/PVDF nanocomposites are successfully prepared by solvothermal method. The electromagnetic absorption performance of Ni_xS_y/PVDF with different filler content is investigated in the range of 2–18 GHz. An optimal reflection loss value of −32.75 dB at 10.48 GHz is achieved for the filler content of 20 wt%, and the bandwidth <-10 dB can reach up to 4.48 GHz with a thickness of 3 mm. Furthermore, fundamental mechanisms of electromagnetic absorbing is discussed, indicating that the interface polarization, electric dipole polarization, Debye relaxation and impedance matching are the main factors affecting the absorption performance of Ni_xS_y/PVDF composites.

Keywords: Ni_xS_y nanoparticles, Ni_xS_y/PVDF nanocomposites, electromagnetic absorption, impedance matching, mechanisms

OPEN ACCESS

Edited by:
Biao Zhao,
Zhengzhou University of Aeronautics, China

Reviewed by:
Long Xia,
Harbin Institute of Technology, China
Fan Wu,
Nanjing University of Science and Technology, China

****Correspondence:***
Mao-Dong Li
2453962572@qq.com
Guang-Sheng Wang
wanggsh@buaa.edu.cn

Specialty section:
This article was submitted to Polymeric and Composite Materials, a section of the journal Frontiers in Materials

Received: *19 February 2020*
Accepted: *18 March 2020*
Published: *21 April 2020*

Citation:
Du Y-H, Gao N, Li M-D, Wang L and Wang G-S (2020) Preparation and Microwave Absorption Properties of Ni_xS_y/PVDF Nanocomposites. Front. Mater. 7:80. doi: 10.3389/fmats.2020.00080

INTRODUCTION

Electromagnetic pollution has been recognized as a new type of pollution in today's society due to the extensive use of electronic equipment and communication technology in commercial, civil and military fields (Yin et al., 2016; Zhan et al., 2018; Zhao Z. et al., 2019). The electromagnetic radiation of various communication devices and electronic instruments seriously threatens the health of human beings, for examples reducing people's energy and physical strength, decreasing the ability of people to remember and think, inducing cancer, as well as producing brain tumors and cardiovascular diseases. And, electromagnetic waves will interfere with each other in space, which causing much damage to the communication system, control failure, and poor communication. In addition, electromagnetic wave leakage can also pose a safety hazard to state secrets (Dai et al., 2018; Feng et al., 2018; Li et al., 2018). In order to reduce the harm of electromagnetic radiation, an effective method is to use electromagnetic wave absorbing material (Liu et al., 2015). The traditional materials limit their practical application due to the high density. Therefore, the new generation absorbing materials should have the characteristics of small thickness, light weight, wide absorption frequency range and strong electromagnetic wave absorption characteristics (Liu et al., 2012; Wu et al., 2016). In recent years, many nanomaterials have been proved to exhibit excellent absorbing properties, such as Fe_3O_4 (Jia et al., 2010), SiC (Kuang et al., 2019), RGO aerogels (Zhang M. et al., 2019), C@CoFeO@MnO_2(Feng et al., 2020), Fe_3O_4@NPC (Xiang et al., 2019), and PbS (Pan et al., 2017). In addition, many studies have shown that most of the nanocomposites have synergistic effects, which will be very beneficial to the absorbing properties of the materials (Liu et al., 2017; Jian et al., 2018; Ma et al., 2018). The typical composites are composed of matrix and filler. Polyvinylidene fluoride (PVDF) is a semi-crystalline material with CH_2-CF_2 repeating unit. Due to its good piezoelectric properties (Mahato et al., 2015), PVDF has been widely studied and

applied as a matrix of composites in the field of wave absorption (Meng et al., 2014; Naseer et al., 2019; Zhao B. et al., 2019).

Transition metal compounds are common absorbers in the field of electromagnetic wave absorption due to their diverse shapes. Lan et al. (2020) designed a novel binary cobalt nickel oxide hollowed-out spheres ($Co_{1.29}Ni_{1.71}O_4$) via facile hydrothermal and calcination method. The $Co_{1.29}Ni_{1.71}O_4$ has a spinel structure, which could improve the dielectric loss and wave absorbing performance of the material under high temperature processing. Sulfide is the most common type of transition metal compound with special band structure and good mechanical properties, which has been extensively applied in solar cells (Wang et al., 2018; Nair et al., 2019), photocatalysis (Yu et al., 2016), lithium batteries (Wu et al., 2015), and sodium ion batteries (Peng et al., 2016) fields. In addition, transition metal sulfide nanomaterials have been widely used as a dielectric loss absorber in the field of absorbing wave due to their dielectric properties. For example, Ning et al. (2015) developed few-layered MoS_2 nanosheets (MoS_2-NS) by the top-down exfoliation method, and the MoS_2-NS composites showed an lower reflection loss (RL) of −38.42 dB when the thickness was 2.4 mm. However, the high density of a single transition metal sulfide material limits its application in real life. Toward this end, it needs to be compounded with other materials to reduce the density of the material and utilize synergy to improve the absorbing properties. Up to now, many composite materials with transition metal sulfide have been studied and used in absorbing wave field, such as PANI/CoS/CDs (Ge et al., 2016), MoS_2/GN (Zhang D. et al., 2018), Ni/ZnS (Zhao et al., 2014), MoS_2/PVDF (Zhang et al., 2016) and so on. However, the microwave absorption properties of Ni_xS_y and its related inorganic-organic composite materials have not been reported. In this study, octahedral Ni_xS_y nanoparticles were synthesized by solvent thermal method and used as fillers to prepare Ni_xS_y/PVDF nanocomposite. The absorption electromagnetic wave performance of Ni_xS_y/PVDF nanocomposites was studied, and the absorbing mechanism was elaborated and analyzed.

EXPERIMENTAL

Materials

All reagents were analytical grade and used without further purification. The preparation of Ni_xS_y is described in the following: 0.3490 g $NiN_2O_6{\cdot}6H_2O$, 0.064 g S powder and 0.24 g PVP were added to 60 ml of ethylene glycol, and the mixture was stirred at room temperature for 1 h. After all the particles were dissolved, the stirring was stopped. And, the reaction kettle was placed in a kettle and placed in an oven. The reaction was carried out at 200°C for 12 h. After cooled to room temperature, the product was washed with water and ethanol, dried for use.

In order to obtain Ni_xS_y/PVDF composite film, an appropriate amount of PVDF was firstly dissolved in 25 mL N-N dimethylformamide (DMF) and stirred for 30 min at room temperature. Then, Ni_xS_y octahedral particles were added, and ultrasonic stirring was performed. After all the solids were dissolved, the solution in the beaker was poured into a watch glass, placed in an oven and dried at 70 *(°C for 3 h. After the mixture was pressed at 210(C (°C for 15 min at 4 MPa. A cylindrical composite film was obtained. In this study, the filler content of samples were set at 10 wt%, 20 wt%, and 30 wt%, respectively.* The preparation process is shown in **Figure 1**.

Characterization

The size and morphologies of Ni_xS_y nanoparticles were tests by scanning electron microscopy (SEM, Quanta 250 FEG). The elemental composition was examined by field emission scanning electron microscopy (FE-SEM, JSM-7500F) with energy dispersive spectrometer (EDS) spectrum and copper grids. The nanomaterials X-ray diffraction (XRD) patterns were collected using a Shimadzu 6000 X-ray diffractometer with Cu Kα radiation (λ = 1.5416 Å) for the Ni_xS_y phase analysis.

Measurements of Electromagnetic Parameters

The cylindrical Ni_xS_y/PVDF with different concentrations were prepared by hot pressing method. The microwave absorption properties of Ni_xS_y/PVDF were measured by two-port vector network analyzer (Agilent N5244a) with coaxial wire setup. The range of measurement was 2–18 GHz.

RESULTS AND DISCUSSION

Figure 2 displays the SEM and FESEM photographs of the Ni_xS_y materials. As shown in **Figure 2a**, Ni_xS_y exhibits an octahedral nanoparticle with a particle size of about 450 nm. From **Figure 2b**, we can find that the elements of Ni and S are uniformly dispersed by scanning the distribution of the elements in the rectangular frame.

In order to obtain the crystal structure of the Ni_xS_y nanoparticles, we tested the samples by XRD. **Figure 3** shows the XRD diffraction pattern of Ni_xS_y nanoparticles. The peaks at the 2q of the asterisk in the figure are 30.34°, 34.88°, and 46.16°, which correspond to the standard card PDF#02-1280 of NiS (Lv et al., 2018). The peaks at the remaining 2q angles correspond exactly to the standard card PDF#11-0099 of the cubic structure of NiS_2 (Zhu et al., 2019).

Supplementary Figure S1 shows the fine-scanned Ni 2p and S 2p XPS spectra of Ni_xS_y. As shown in **Supplementary Figure S1A**, the peaks at 855.7 and 853.5 eV are assigned to Ni $2p_{1/2}$ and Ni $2p_{3/2}$ of Ni^{2+}, 871.9 and 874.2 eV were assigned to Ni $2p_{3/2}$ and Ni $2p_{1/2}$ of Ni^{3+}. The Ni 2p spectra evidence the formation of NiS_2 (Yang et al., 2016). **Supplementary Figure S1B** shows the S 2p XPS spectra. The peaks at 161.54 and 162.4 eV are attributed to S $2p_{3/2}$ and S $2p_{1/2}$ of Ni-S bonding, while the peaks at 163.5 and 167.8 eV correspond to the S_2^{2-} and sulfates with high oxidation state. The XPS analyses point out the formation of Ni_xS_y.

In order to study the absorbing properties of Ni_xS_y/PVDF nanocomposites, the samples with different filler content were tested by the coaxial method in the range of 2–18 GHz. The permittivity and magnetic permeability of each sample can be obtained. **Figure 4A** shows the RL curves of four

FIGURE 1 | Experimental preparation flow chart.

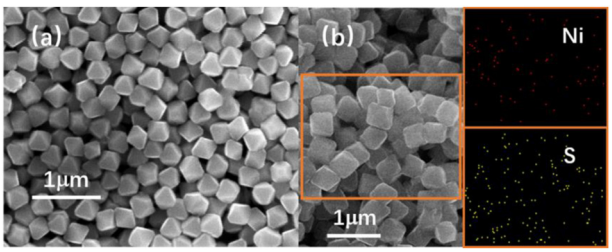

FIGURE 2 | (a) SEM photograph of Ni_xS_y nanoparticles; **(b)** FESEM photograph and energy spectra of Ni and S elements.

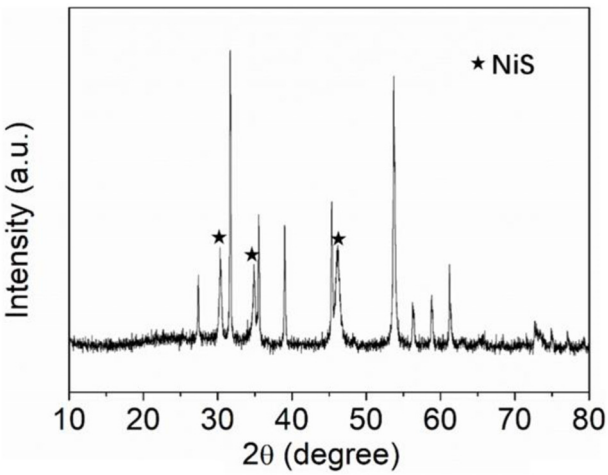

FIGURE 3 | XRD pattern of Ni_xS_y nanomaterials.

samples at a thickness of 3 mm. It can be seen that the RL value of Ni_xS_y/PVDF composite is −9.8 dB at 6.1 GHz. By comparing the RL values of paraffin composites and Ni_xS_y/PVDF composite materials, we can see that Ni_xS_y/PVDF have much better absorbing effect than that of paraffin composites. The Ni_xS_y/PVDF nanocomposites with a filler content of 20 wt% have the optimal RL value of −32.75 dB and a broad effective bandwidth of 4.48 GHz. **Figure 4B** shows the RL of the material at different thicknesses when the filler content is 20 wt%. It is clear that the thickness is also a key factor affecting the absorbing properties of the material. **Figures 4C,D** show three-dimensional maps of Ni_xS_y/PVDF nanocomposites with filler content of 10 and 30 wt%, respectively. Compared with Ni_xS_y/wax, the absorbing properties of Ni_xS_y/PVDF are significantly improved, further demonstrating that compounding with PVDF can increase the electromagnetic wave absorption properties of the material.

Figures 5A,B show the variation of the dielectric real (ε') and imaginary (ε″) of the four materials with frequency. It can be seen that the ε' and ε″ ratios of the nanomaterials composited with PVDF are larger than the ε' and ε″ of the paraffin-composited materials, and the real and imaginary dielectric parts of the sample compounded with PVDF enhance with the increase of filling concentration. As the number of Ni_xS_y nanoparticles increases, more dielectric polarization occurs inside the material. And polarization causes polarization relaxation, so more polarization leads to an increase in ε″. As the frequency increases, the real and imaginary parts of the dielectric remain almost stable, because the increase in frequency causes the rotational speed of the internal electric dipole of the material to keep up with the frequency of the external alternating electromagnetic field (Ohlan et al., 2010).

As known, Ni_xS_y nanoparticles are semiconductor materials, so there is only dielectric loss in the material without magnetic loss, and interfacial polarization exists between adjacent two phases with different dielectric constant and conductivity (Dai et al., 2017). Due to the complexation of Ni_xS_y nanoparticles with PVDF, there is interfacial polarization in the material (**Figure 6**). The relaxation phenomenon caused by the polarization of the interface converts the electromagnetic energy into thermal energy, which contributes to the improvement of the absorbing ability of the material (Roy and Bera, 2012). In addition, PVDF is a polar material because it contains F atoms. The positive and negative charge centers of polar molecules do not coincide, so there is an electric dipole moment (Xu et al., 2018). When an alternating electric field is applied to such a polar material, a galvanic couple occurs in the material. Polarization of the poles would further contribute to the loss of electromagnetic energy (Chen et al., 2009). When the filler content increases, that is, the surface of the Ni_xS_y nanoparticles in the polymer increase, the interfacial polarization increases, and the real and imaginary parts of the dielectric constant increase. However, the dielectric constant is too high to allow

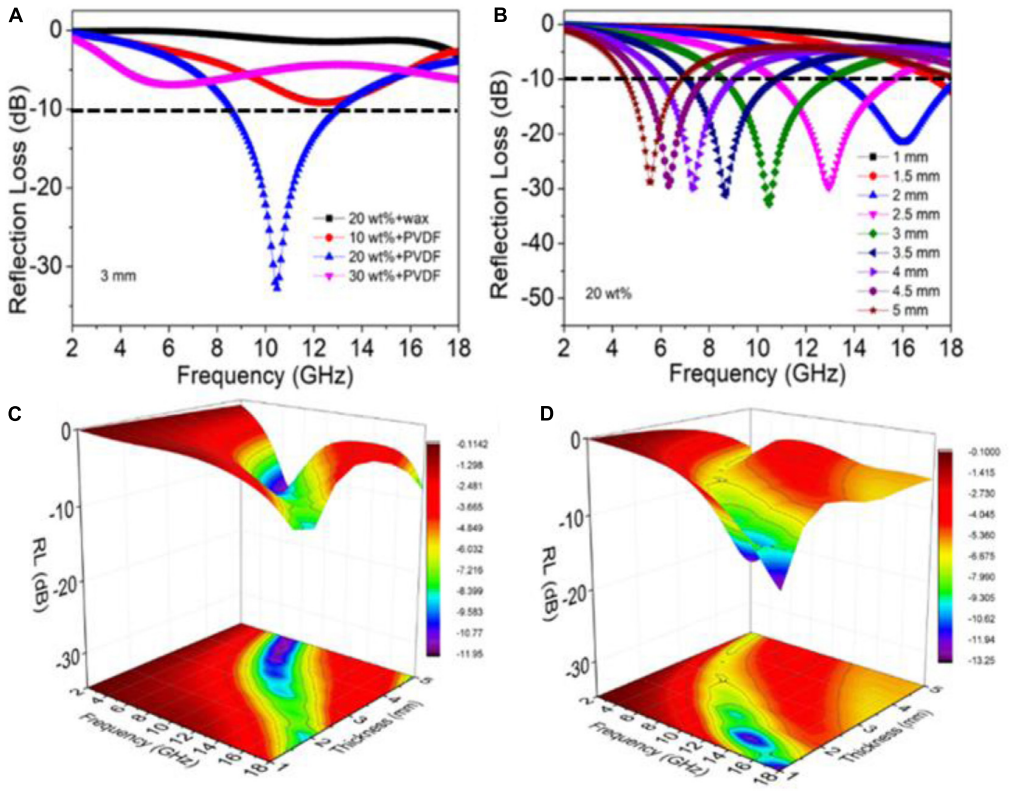

FIGURE 4 | (A) Reflection loss values of four samples at a thickness of 3 mm; **(B)** reflection loss values at different thicknesses of Ni_xS_y/PVDF nanocomposites with a filler content of 20 wt%; **(C)** Ni_xS_y at a filler content of 10 wt% 3D map of /PVDF nanocomposites; **(D)** 3D map of Ni_xS_y/PVDF nanocomposites with a filler content of 30 wt%.

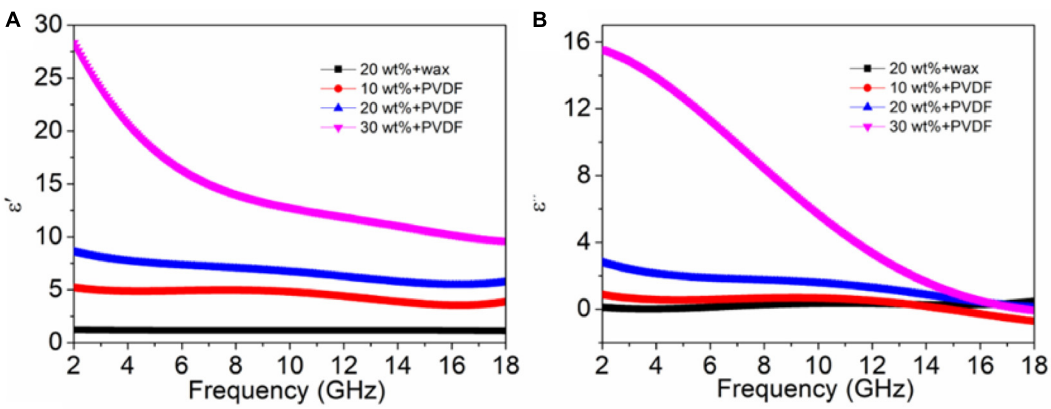

FIGURE 5 | Four composite materials **(A)** dielectric real part; **(B)** dielectric imaginary part.

the material to meet the dielectric matching, so that the electromagnetic wave cannot completely enter the interior of the material and affect its absorption of electromagnetic waves. As a result, the composite with 20% filler content achieves the best absorbing property.

In addition, Debye relaxation is another important dielectric loss mechanism. As the electric field in the medium changes, the delay of molecular polarization causes the relaxation process to occur. If the Debye relaxation behavior is considered, the relative complex permittivity can be expressed as follows (Dong et al., 2008; Shi et al., 2016):

$$\varepsilon_r = \varepsilon_\infty + \frac{\varepsilon_s - \varepsilon_\infty}{1 + j2\pi f\tau} = \varepsilon' - j\varepsilon \quad (1)$$

$$\varepsilon' = \varepsilon_\infty + \frac{\varepsilon_s - \varepsilon_\infty}{1 + (2\pi f)^2\tau^2} \quad (2)$$

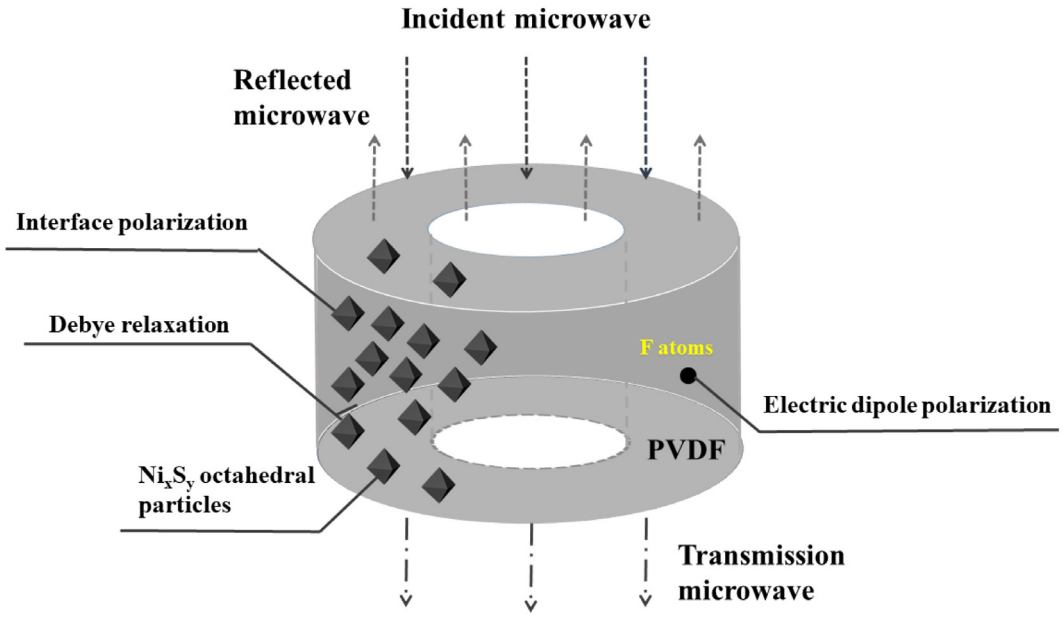

FIGURE 6 | Possible mechanisms of microwave absorption for cylindrical Ni_xS_y/PVDF composites.

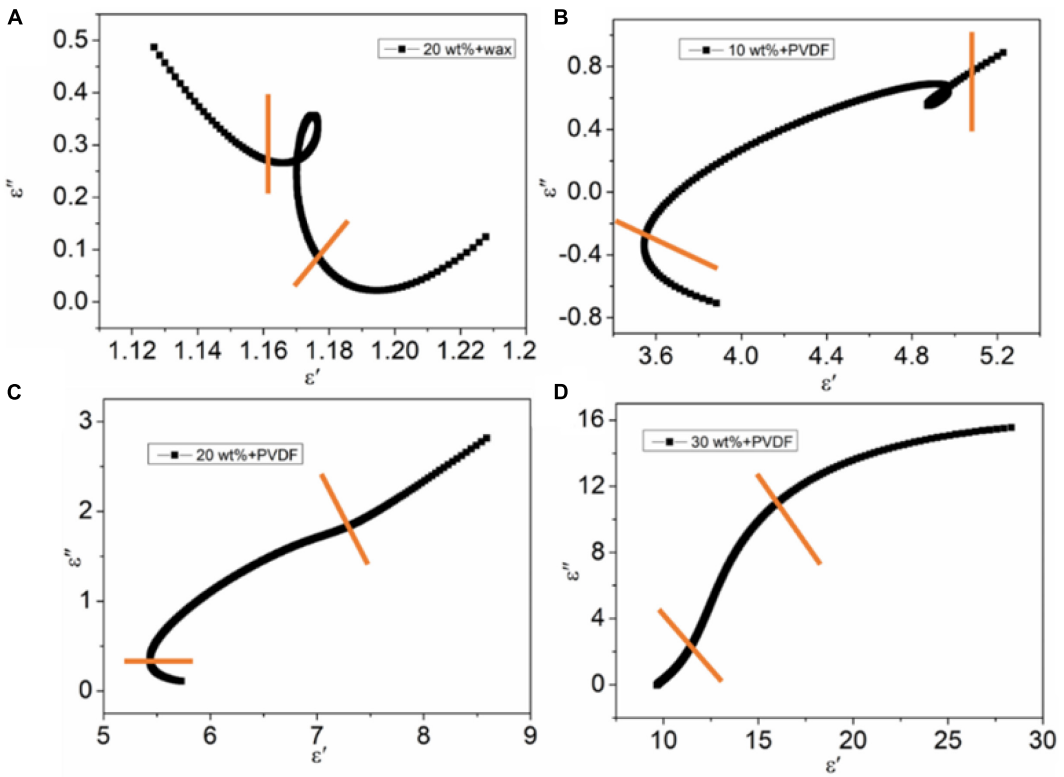

FIGURE 7 | (A) ε′-ε″ curve of Ni_xS_y/wax composite with a filler content of 20 wt%; filler content is **(B)** 10 wt%; **(C)** 20 wt%; and **(D)** 30 wt% of the ε′-ε″ curve of Ni_xS_y/PVDF nanocomposites.

TABLE 1 | Electromagnetic wave absorption properties of various composite materials including transition metal compound nanomaterials in previous reports compared with this work.

Absorber	Matrix	Content (wt%)	RL_{min} (dB)	d (mm)	EAB(GHz) (RL < −10 dB)	References
SiC nanowires	Paraffin	40	−35.2	1.3	1.8	Kuang et al., 2019
Ni@NCNTs	Paraffin	10	−34.1	3.2	4.7	Zhang J. et al., 2019
Ni/ZnS	Paraffin	–	−25.78	2.7	4.72	Zhao et al., 2014
Fe/C	Paraffin	15	−29.5	2.5	4.3	Liu et al., 2017
MoS_2-NS	Paraffin	60	−38.42	2.4	4.1	Ning et al., 2015
$La_{0.8}FeO_3$/C/RGO-BD	Paraffin	30	−42.69	3.15	2.72	Jia et al., 2019
$MgCo_2O_4/Co_3O_4$	Paraffin	50	−48.54	2.3	5.08	Liu et al., 2019
TiN/RGO	Paraffin	2	−42.85	4.0	6.7	Wei et al., 2019
MoS_2/PVDF	PVDF	20	−32.67	3.5	4.4	Zhang et al., 2016
hollow $Co_{1-x}S$ microspheres	PVDF	3	−46.1	2.55	5.6	Zhang X.J. et al., 2018
MoO_3/MoS_2	PVDF	20	−38.5	2.0	2.0	Li et al., 2019
Ni_xS_y/PVDF	PVDF	20	−32.75	3.0	4.48	This work

$$\varepsilon'' = \frac{(\varepsilon_s - \varepsilon_\infty)2\pi f\tau}{1 + (2\pi f)^2\tau^2} \quad (3)$$

Where f is the frequency, ε_s is the dielectric constant in the DC dielectric, and ε_∞ is the relative dielectric constant of the high frequency limit. Based on Equations (2) and (3), the relationship between ε' and ε'' can be inferred as follows:

$$\left(\varepsilon' - \frac{\varepsilon_s - \varepsilon_\infty}{2}\right)^2 + (\varepsilon'')^2 = \left(\frac{\varepsilon_s - \varepsilon_\infty}{2}\right)^2 \quad (4)$$

Among them, we find that the curve ε'-ε'' is a semicircle. If Debye relaxation occurs, a semicircle will appear in the image. It can be seen from **Figures 7A–D** that there are two half rings in the ε'-ε'' curve of the four materials, which proves the existence of the Debye relaxation loss mechanism. For the Ni_xS_y/wax composites, the relaxation peak mainly results from dipolar polarization (Lv et al., 2018). And two semicircles illustrate the double dielectric relaxation processes in Ni_xS_y/PVDF composites. When the filler content increases, the Cole-Cole plot is close to a straight line, which means that the conductivity loss plays the main role in the dielectric loss process and the polarization no longer occupies the first status. The Debye relaxation process has been hidden because of the enhanced electrical conductivity. The higher conductivity can lead to skin effect that inhibits the further incidence of microwaves into the absorbers (Zhu et al., 2019), which is the reason that high filler rate will reduce the absorbing performance of the composite.

Based on these results, it can be concluded that the mechanism of Ni_xS_y/PVDF may be interface polarization, electric dipole polarization, Debye relaxation and impedance matching. When the electromagnetic wave entering the absorber, the polyhedral structure of Ni_xS_y nanoparticles causes interfacial polarization at its interface with PVDF, and the relaxation caused by interfacial polarization improves the absorbing performance of the composite. In addition, there is a dipole in the polar material PVDF, which causes galvanic polarization after the electromagnetic wave is incident. Debye relaxation is another important dielectric loss pathway caused by the delay in molecular polarization. The synergistic effect of different mechanisms increases the dielectric loss of the composite material, so that Ni_xS_y / PVDF composite material has excellent absorption properties. **Table 1** summarizes electromagnetic wave absorption properties of various composite materials including transition metal compound nanomaterials reported in literature. Ni_xS_y/PVDF prepared in this work has the advantages of low filler content, thinner thickness and broadening efficient absorption bandwidth.

CONCLUSION

Transition metal sulfide nanomaterials have been widely used and studied as a dielectric loss absorbing material in the field of absorbing wave due to their dielectric properties. The high density of a single transition metal sulfide material limits its application in real life. For this reason, it needs to be compounded with other materials to reduce the density of the material, and the synergy between different materials is used to improve the absorbing properties. In this paper, octahedral Ni_xS_y nanoparticles with excellent dispersibility were prepared by solvothermal method and combined with PVDF. The Ni_xS_y/PVDF nanocomposites with different filler content were measured by coaxial method in the range of 2–18 GHz. The measurement results show that the material has the best absorption performance when the filler content is 20 wt%, the maximum reflection loss is up to −32.75 dB, and the absorption frequency band width is 4.48 GHz. Through the analysis of dielectric constant and absorption mechanism, the composite material of octahedral Ni_xS_y and PVDF has interface polarization, electric dipole polarization, Debye relaxation, and appropriate impedance matching.

DATA AVAILABILITY STATEMENT

All datasets generated for this study are included in the article/**Supplementary Material**.

AUTHOR CONTRIBUTIONS

Y-HD and NG: data curation and writing-original draft preparation. LW: conceptualization, methodology, visualization, and investigation. M-DL and G-SW: supervision.

FUNDING

This work was supported by the National Natural Science Foundation of China (No. 51672013), the Fundamental Research Funds for the Central Universities, the Guangdong Science and Technology Project: 2019A101002036 and Science and Technology Project of Guangdong Municipal Bureau of Market Supervision: 2018CZ16.

SUPPLEMENTARY MATERIAL

The Supplementary Material for this article can be found online at: https://www.frontiersin.org/articles/10.3389/fmats.2020.00080/full#supplementary-material

REFERENCES

Chen, Y. J., Gao, P., Wang, R. X., Zhu, C. L., Wang, L. J., Cao, M. S., et al. (2009). Porous Fe3O4/SnO2 core/shell nanorods: synthesis and electromagnetic properties. *J. Phys. Chem C* 113, 10061–10064. doi: 10.1021/jp902296z

Dai, B., Zhao, B., Xie, X., Su, T., Fan, B., Zhang, R., et al. (2018). Novel two-dimensional Ti 3C2Tx MXenes/nano-carbon sphere hybrids for high-performance microwave absorption. *J. Mater. Chem. C* 6, 5690–5697. doi: 10.1039/C8TC01404C

Dai, S., Zhao, B., Qu, C., Chen, D., Dang, D., Song, B., et al. (2017). Controlled synthesis of three-phase NixSy/rGO nanoflake electrodes for hybrid supercapacitors with high energy and power density. *Nano Energy*. 33, 522–531. doi: 10.1016/j.nanoen.2017.01.056

Dong, X., Zhang, X., Huang, H., and Zuo, F. (2008). Enhanced microwave absorption in Ni/polyaniline nanocomposites by dual dielectric relaxations. *Appl. Phys. Lett.* 92:013127. doi: 10.1063/1.2830995

Feng, A., Hou, T., Jia, Z., and Wu, G. (2020). Synthesis of hierarchical carbon fiber@cobalt ferrite@manganese dioxide composite and its application as microwave absorber. *RSC Adv.* 10, 10510–10518. doi: 10.1039/c9ra10327a

Feng, A., Jia, Z., Zhao, Y., and Lv, H. (2018). Development of Fe/Fe3O4@ C composite with excellent electromagnetic absorption performance. *J. Alloys Compd.* 745, 547–554. doi: 10.1016/j.jallcom.2018.02.255

Ge, C., Zhang, X., Liu, J., Jin, F., Liu, J., and Bi, H. (2016). Hollow-spherical composites of Polyaniline/Cobalt Sulfide/Carbon nanodots with enhanced magnetocapacitance and electromagnetic wave absorption capabilities. *Appl. Surf. Sci.* 378, 49–56. doi: 10.1016/j.apsusc.2016.03.210

Jia, K., Zhao, R., Zhong, J., and Liu, X. (2010). Preparation and microwave absorption properties of loose nanoscale Fe3O4 spheres. *J. Magn. Magn. Mater.* 322, 2167–2171. doi: 10.1016/j.jmmm.2010.02.003

Jia, Z., Gao, Z., Feng, A., Zhang, Y., Zhang, C., Nie, G., et al. (2019). Laminated microwave absorbers of A-site cation deficiency perovskite La0. 8FeO3 doped at hybrid RGO carbon. *Compos. Part B Eng.* 176:107246. doi: 10.1016/j.compositesb.2019.107246

Jian, X., Xiao, X., Deng, L., Tian, W., Wang, X., Mahmood, N., et al. (2018). Heterostructured nanorings of Fe-Fe3O4@C hybrid with enhanced microwave absorption performance. *ACS Appl. Mater. Inter.* 10, 9369–9378. doi: 10.1021/acsami.7b18324

Kuang, J., Xiao, T., Hou, X., Zheng, Q., Wang, Q., Jiang, P., et al. (2019). Microwave synthesis of worm-like SiC nanowires for thin electromagnetic wave absorbing materials. *Ceram. Int.* 45, 11660–11667. doi: 10.1016/j.ceramint.2019.03.040

Lan, D., Qin, M., Liu, J., Wu, G., Zhang, Y., and Wu, H. (2020). Novel binary cobalt nickel oxide hollowed-out spheres for electromagnetic absorption applications. *Chem. Eng. J.* 382:122797. doi: 10.1016/j.cej.2019.122797

Li, C. Q., Shen, X., Ding, R. C., and Wang, G. S. (2019). Controllable synthesis of one-dimensional MoO3/MoS2 hybrid composites with their enhanced efficient electromagnetic wave absorption properties. *Chempluschem* 84, 226–232. doi: 10.1002/cplu.201800599

Li, J., Xie, Y., Lu, W., and Chou, T. W. (2018). Flexible electromagnetic wave absorbing composite based on 3D rGO-CNT-Fe3O4 ternary films. *Carbon* 129, 76–84. doi: 10.1016/j.carbon.2017.11.094

Liu, J., Che, R., Chen, H., Zhang, F., Xia, F., Wu, Q., et al. (2012). Microwave absorption enhancement of multifunctional composite microspheres with spinel Fe3O4 cores and anatase TiO2 shells. *Small* 8, 1214–1221. doi: 10.1002/smll.201102245

Liu, J., Liang, H., Zhang, Y., Wu, G., and Wu, H. (2019). Facile synthesis of ellipsoid-like MgCo2O4/Co3O4 composites for strong wideband microwave absorption application. *Compos. Part B Eng.* 176:107240. doi: 10.1016/j.compositesb.2019.107240

Liu, Q., Liu, X., Feng, H., Shui, H., and Yu, R. (2017). Metal organic framework-derived Fe/carbon porous composite with low Fe content for lightweight and highly efficient electromagnetic wave absorber. *Chem. Eng. J.* 314, 320–327. doi: 10.1016/j.cej.2016.11.089

Liu, X., Wu, N., Cui, C., Bi, N., and Sun, Y. (2015). One pot synthesis of Fe3O4/MnO2 core–shell structured nanocomposites and their application as microwave absorbers. *RSC Adv.* 5, 24016–24022. doi: 10.1039/C4RA14753G

Lv, J., Cheng, Y., Liu, W., Quan, B., Liang, X., Ji, G., et al. (2018). Achieving better impedance matching by a sulfurization method through converting Ni into NiS/Ni3S4 composites. *J. Mater. Chem. C* 6, 1822–1828. doi: 10.1039/C7TC05503J

Ma, J., Wang, X., Cao, W., Han, C., Yang, H., Yuan, J., et al. (2018). A facile fabrication and highly tunable microwave absorption of 3D flower-like Co3O4-rGO hybrid-architectures. *Chem. Eng. J.* 339, 487–498. doi: 10.1016/j.cej.2018.01.152

Mahato, P., Seal, A., Garain, S., and Sen, S. (2015). Effect of fabrication technique on the crystalline phase and electrical properties of PVDF films. *Mater. Sci. Poland* 33, 157–162. doi: 10.1515/msp-2015-0020

Meng, X. M., Zhang, X. J., Lu, C., Pan, Y. F., and Wang, G. S. (2014). Enhanced absorbing properties of three-phase composites based on a thermoplastic-ceramic matrix (BaTiO3+ PVDF) and carbon black nanoparticles. *J. Mater. Chem. A* 2, 18725–18730. doi: 10.1039/C4TA04493B

Nair, P., Medina, E. A. Z., García, G. V., Martínez, L. G., and Nair, M. (2019). Functional prototype modules of antimony sulfide selenide thin film solar cells. *Thin. Solid Films* 669, 410–418. doi: 10.1016/j.tsf.2018.11.019

Naseer, A., Mumtaz, M., Raffi, M., Ahmad, I., Khan, S. D., Shakoor, R. I., et al. (2019). Reinforcement of electromagnetic wave absorption characteristics in PVDF-PMMA nanocomposite by intercalation of carbon nanofibers. *Electron. Mater. Lett.* 15, 201–207. doi: 10.1007/s13391-018-00104-9

Ning, M. Q., Lu, M. M., Li, J.-B., Chen, Z., Dou, Y. K., Wang, C. Z., et al. (2015). Two-dimensional nanosheets of MoS2: a promising material with high dielectric properties and microwave absorption performance. *Nanoscale* 7, 15734–15740. doi: 10.1039/C5NR04670J

Ohlan, A., Singh, K., Chandra, A., and Dhawan, S. K. (2010). Microwave absorption behavior of core-shell structured poly (3, 4-ethylenedioxy thiophene)-barium ferrite nanocomposites. *ACS Appl. Mater. Inter.* 2, 927–933. doi: 10.1021/am900893d

Pan, Y. F., Wang, G. S., Liu, L., Guo, L., and Yu, S. H. (2017). Binary synergistic enhancement of dielectric and microwave absorption properties: a composite of arm symmetrical PbS dendrites and polyvinylidene fluoride. *Nano Res.* 10, 284–294. doi: 10.1007/s12274-016-1290-8

Peng, S., Han, X., Li, L., Zhu, Z., Cheng, F., Srinivansan, M., et al. (2016). Unique cobalt sulfide/reduced graphene oxide composite as an anode for sodium-ion batteries with superior rate capability and long cycling stability. *Small* 12, 1359–1368. doi: 10.1002/smll.201502788

Roy, P., and Bera, J. (2012). Study on electromagnetic properties of MgCuZn ferrite/BaTiO3 composites. *Mater. Chem. Phys.* 132, 354–357. doi: 10.1016/j.matchemphys.2011.11.031

Shi, G., Zhang, B., Wang, X., and Fu, Y. (2016). Enhanced microwave absorption properties of core double-shell type Fe@C@BaTiO3 nanocapsules. *J. Alloys Compd.* 655, 130–137. doi: 10.1016/j.jallcom.2015.09.147

Wang, X., Tang, R., Wu, C., Zhu, C., and Chen, T. (2018). Development of antimony sulfide–selenide Sb2(S,Se)3-based solar cells. *J. Energy Chem.* 27, 713–721. doi: 10.1016/j.jechem.2017.09.031

Wei, Y., Shi, Y., Jiang, Z., Zhang, X., Chen, H., Zhang, Y., et al. (2019). High performance and lightweight electromagnetic wave absorbers based on TiN/RGO flakes. *J. Alloys Compd.* 810:151950. doi: 10.1016/j.jallcom.2019.151950

Wu, R., Wang, D. P., Rui, X., Liu, B., Zhou, K., and Chen, Z. (2015). In-situ formation of hollow hybrids composed of cobalt sulfides embedded within porous carbon polyhedra/carbon nanotubes for high-performance lithium-ion batteries. *Adv. Mater.* 27, 3038–3044. doi: 10.1002/adma.201500783

Wu, T., Liu, Y., Zeng, X., Cui, T., Zhao, Y., Li, Y., et al. (2016). Facile hydrothermal synthesis of Fe3O4/C core–shell nanorings for efficient low-frequency microwave absorption. *ACS Appl. Mater. Inter.* 8, 7370–7380. doi: 10.1021/acsami.6b00264

Xiang, Z., Song, Y., Xiong, J., Pan, Z., Wang, X., Liu, L., et al. (2019). Enhanced electromagnetic wave absorption of nanoporous Fe3O4@carbon composites derived from metal-organic frameworks. *Carbon* 142, 20–31. doi: 10.1016/j.carbon.2018.10.014

Xu, W., Pan, Y. F., Wei, W., Wang, G. S., and Qu, P. (2018). Microwave absorption enhancement and dual-nonlinear magnetic resonance of ultra small nickel with quasi-one-dimensional nanostructure. *Appl. Surf. Sci.* 428, 54–60. doi: 10.1016/j.apsusc.2017.09.052

Yang, N., Tang, C., Wang, K., Du, G., Asiri, A. M., and Sun, X. (2016). Iron-doped nickel disulfide nanoarray: a highly efficient and stable electrocatalyst for water splitting. *Nano Res.* 9, 3346–3354. doi: 10.1007/s12274-016-1211-x

Yin, Y., Liu, X., Wei, X., Yu, R., and Shui, J. (2016). Porous CNTs/Co composite derived from zeolitic imidazolate framework: a lightweight, ultrathin, and highly efficient electromagnetic wave absorber. *ACS Appl. Mater. Inter.* 8, 34686–34698. doi: 10.1021/acsami.6b12178

Yu, H., Xiao, P., Wang, P., and Yu, J. (2016). Amorphous molybdenum sulfide as highly efficient electron-cocatalyst for enhanced photocatalytic H2 evolution. *Appl. Catal. B Environ.* 193, 217–225. doi: 10.1016/j.apcatb.2016.04.028

Zhan, Y., Long, Z., Wan, X., Zhang, J., He, S., and He, Y. (2018). 3D carbon fiber mats/nano-Fe3O4 hybrid material with high electromagnetic shielding performance. *Appl. Surf. Sci.* 444, 710–720. doi: 10.1016/j.apsusc.2018.03.006

Zhang, D., Jia, Y., Cheng, J., Chen, S., Chai, J., Yang, X., et al. (2018). High-performance microwave absorption materials based on MoS2-graphene isomorphic hetero-structures. *J. Alloys Compd.* 758, 62–71. doi: 10.1016/j.jallcom.2018.05.130

Zhang, X. J., Zhu, J. Q., Yin, P. G., Guo, A. P., Huang, A. P., Guo, L., et al. (2018). Tunable high-performance microwave absorption of Co1–xS hollow spheres constructed by nanosheets within ultralow filler loading. *Adv. Funct. Mater.* 28:1800761. doi: 10.1002/adfm.201800761

Zhang, J., Shu, R., Guo, C., Sun, R., Chen, Y., and Yuan, J. (2019). Fabrication of nickel ferrite microspheres decorated multi-walled carbon nanotubes hybrid composites with enhanced electromagnetic wave absorption properties. *J. Alloys Compd.* 784, 422–430. doi: 10.1016/j.jallcom.2019.01.073

Zhang, M., Jiang, Z., Lv, X., Zhang, X., Zhang, Y., Zhang, J., et al. (2019). Microwave absorption performance of reduced graphene oxide with negative imaginary permeability. *J. Phys. D Appl. Phys.* 53:02LT01. doi: 10.1088/1366-6463/ab48a7

Zhang, X. J., Li, S., Wang, S. W., Yin, Z. J., Zhu, J. Q., Guo, A. P., et al. (2016). Self-supported construction of three-dimensional MoS2 hierarchical nanospheres with tunable high-performance microwave absorption in broadband. *J. Phys. Chem. C* 120, 22019–22027. doi: 10.1021/acs.jpcc.6b06661

Zhao, B., Deng, J., Zhao, C., Wang, C., Chen, Y. G., Hamidinejad, M., et al. (2019). Achieving wideband microwave absorption properties in PVDF nanocomposite foams with an ultra-low MWCNT content by introducing a microcellular structure. *J. Mater. Chem. C* 8, 58–70. doi: 10.1039/C9TC04575A

Zhao, Z., Xu, S., Du, Z., Jiang, C., and Huang, X. (2019). Metal–organic framework-based PB@ MoS2 core–shell microcubes with high efficiency and broad bandwidth for microwave absorption performance. *ACS Sustain. Chem. Eng.* 7, 7183–7192. doi: 10.1021/acssuschemeng.9b00191

Zhao, B., Shao, G., Fan, B., Zhao, W., Xie, Y., and Zhang, R. (2014). ZnS nanowall coated Ni composites: facile preparation and enhanced electromagnetic wave absorption. *RSC Adv.* 4, 61219–61225. doi: 10.1039/C4RA08095E

Zhu, W., Zhang, L., Zhang, W., Zhang, F., Li, Z., Zhu, Q., et al. (2019). Facile synthesis of GNPs@ NixSy@ MoS2 composites with hierarchical structures for microwave absorption. *Nanomaterials* 9:1403. doi: 10.3390/nano9101403

Conflict of Interest: The authors declare that the research was conducted in the absence of any commercial or financial relationships that could be construed as a potential conflict of interest.